Journal of The Electrochemical Society, **161** (8) E3323-E3327 (2014)
0013-4651/2014/161(8)/E3323/5/$31.00 © The Electrochemical Society

JES Focus Issue on Mathematical Modeling of Electrochemical Systems at Multiple Scales

Effective Macroscopic Equations for Species Transport and Reactions in Porous Catalyst Layers

M. Schmuck[a,z] and Peter Berg[b,*,z]

[a]*School of Mathematical and Computer Sciences, and the Maxwell Institute for Mathematical Sciences, Heriot-Watt University, Edinburgh EH14 4AS, United Kingdom*
[b]*Department of Physics, Norwegian University of Science and Technology, 7491 Trondheim, Norway*

A macroscopic model for a porous catalyst layer is derived from a microscopic description that includes the reduction of oxygen in periodically distributed pores filled with liquid water. While specific transport equations are established for a cathode catalyst layer in a PEM fuel cell, the same multi-scale approach would yield governing equations for other types of electrodes which are mathematically analogous. Macroscopic transport characteristics such as porous media (corrector) tensors, Darcy's law and an effective Butler-Volmer equation, are inherently linked to the dynamics at the microscale and can be computed in a fairly straightforward manner under the assumption of local thermodynamic equilibrium. In the case of periodic and strongly convective flows, we also obtain so-called diffusion-dispersion relations, e.g. Taylor-Aris dispersion.

Manuscript submitted February 6, 2014; revised manuscript received June 2, 2014. Published June 12, 2014. *This paper is part of the JES Focus Issue on Mathematical Modeling of Electrochemical Systems at Multiple Scales.*

As the world's energy economy moves away from fossil fuels, efficient electrochemical conversion of other types of fuel is becoming increasingly important.[12] While many factors determine the efficiency of such processes, electrode design appears to be the dominant element.[22] Optimal electrode design is essential for many applications and it has lately received particular attention in relation to energy conversion devices such as batteries and fuel cells.

For polymer electrolyte membrane (PEM) fuel cells (FCs), the focus lies on the design of efficient, cost effective and durable catalyst layers (CLs),[4] especially at the cathode side where the relatively inefficient oxygen reduction reaction (ORR)

$$O_2 + 4H^+ + 4e^- \rightarrow 2H_2O \qquad [1.1]$$

takes place. Consequently, the cathode CL is responsible for the major portion of voltage losses. Usually, it is a random porous medium[13] whose material properties and performance characteristics are dictated by its manufacturing process. A systematic optimization of this multi-phase medium is extremely challenging, owing to a pore-size distribution that can hardly be controlled which results in non-optimal performance. Since PEMFC research and development should ideally guide, and not be guided by, the production process in terms of geometry, morphology and materials, there is a need to move toward new materials and design tools, based on simulation models with predictive capabilities.

One idea is to enhance the development of rational designs for new and optimized, ordered CL nanostructures, as opposed to random media.[4] Advances in nanoscale manufacturing and in the synthesis of porous electrodes increasingly facilitate the fabrication of tailored catalyst layers with periodic pore structures.[8,21] These catalyst layers can be ultra thin and made from organic perylene whiskers,[8] carbon nanotubes or fibers,[21] or mesoporous carbon,[21] for example. However, this development needs to be supported by the employment of mathematical models, simulation and optimization techniques related to the scaling up of the dynamics at the microscale so as to assess and predict the macroscopic performance of such new devices.[10,18]

In principle, a rigorous upscaling should start at the molecular level but molecular dynamics (MD) simulations are still restricted in terms of system size, owing to a lack of computing power and speed on today's high-performance computing clusters. Typically, MD simulations do not go beyond the single pore level.[15] Moreover, the inclusion of electro-chemical reactions into MD simulations further complicates the matter which is also one reason why coarse-grained methods, like dissipative particle dynamics (DPD) simulations,[23] are problematic alternatives for proper upscaling.

Instead, this work employs a continuum approach, using the well-known Poisson-Nernst-Planck (PNP) equations, coupled to (Navier-) Stokes (NS) flow, assuming a fully flooded electrode.[5,18] While our mathematical approach is applicable to many porous electrodes and electrochemical reactions, we will focus on the oxygen reduction reaction in PEM fuel cells,[5] described by Eq. (1.1). In particular, we consider an electron-conducting carbon matrix that forms a thin porous structure whose walls are uniformly covered with a catalyst, for example platinum. The pores are filled with liquid water, the product of the ORR, that contains oxygen and protons which react at the pore surface. In contrast, ionomers are absent in such ultra-thin catalyst layers (UTCLs).[5] Since platinum use in PEM fuel cells needs to drop by an order of magnitude so as to make CLs cost effective, it is vital to have reliable and powerful transport models to better understand CL performance and functionality. For these reasons, these models should go beyond simple volume averaging and treat nonlinearities in a rigorous manner.

This contribution begins in the next section with a model description of the reaction kinetics at the microscopic pore level. It extends previous work[18] to include the flow of water through the porous electrode. Subsequently, the model equations are scaled up to the macroscopic level by use of asymptotic multi-scale expansions. Only the main results and steps are presented for reasons of readability, given the highly technical nature of this upscaling technique. The derivation extends the detailed examination in 18, which explains thoroughly the upscaling by homogenization for periodic catalyst layers, toward the crucial influence of fluid flow. As a result, we obtain effective macroscopic transport equations for periodic catalyst layers in the case of general Stokes flows. Additionally, in the case of periodic and strongly convective flows, we also obtain so-called diffusion-dispersion relations (e.g. Taylor-Aris dispersion). The main feature of our result is that our asymptotic multi-scale approach systematically leads to effective porous media correction tensors such as effective diffusion, mobility and electro-permeability coefficients that reliably account for the pore geometry on the microscale. We then conclude with a summary of the results.

Microscopic Transport Equations for Porous Catalysts

In this work, we present two methodologies which allow us to extend the framework introduced in Schmuck and Berg,[18] where fluid flow was entirely neglected, toward equations accounting for periodic or strongly convective flows described by the incompressible Stokes

*Electrochemical Society Active Member.
[z]E-mail: M.Schmuck@hw.ac.uk; peter.berg@ntnu.no

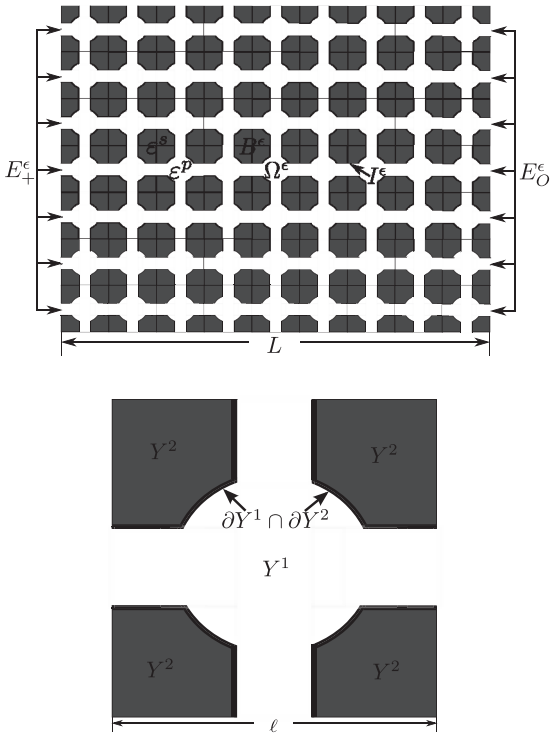

Figure 1. Top. Microscopic (pore-scale) representation of the catalyst layer: Ω^ϵ pore phase, B^ϵ solid phase, $I^\epsilon := \partial\Omega^\epsilon \cap \partial B^\epsilon$ pore walls, E^ϵ_O entrance for O_2, and E^ϵ_+ entrance for H^+. ε^p and ε^s are the electric permittivities of the pore and solid phase, respectively. **Bottom.** Reference cell defining the pore geometry: Y^1 pore phase, Y^2 solid phase, $I_Y := \partial Y^1 \cap \partial Y^2$ pore walls.

equation (by a moving frame strategy) as well as a reaction-diffusion-Darcy-type formulation (by two-scale asymptotics). First, we introduce the general notation required to formulate the basic transport equations on the pore-scale, which we refer to as the microscale. The macroscopic porous catalyst layer $\Omega \subset \mathbb{R}^N$ shall be an open bounded domain. The variable $1 \le N \le 3$ is the dimension of space. On the pore-scale, we denote the solid phase/matrix by $B^\epsilon \subset \Omega$ and the pore phase by Ω^ϵ such that the macroscopic porous catalyst layer is composed as follows $\Omega := \Omega^\epsilon \cup B^\epsilon$, see Figure 1. The parameter $\epsilon := \frac{\ell}{L}$ defines the heterogeneity for the characteristic length scale ℓ of a reference pore $Y \subset \mathbb{R}^N$ and for the macroscopic length scale of the porous catalyst, L. In our subsequent mathematical analysis, we will focus on strongly heterogeneous catalyst materials, i.e. $\epsilon \ll 1$. The reference cell itself is composed of a solid phase Y^2 and a pore phase Y^1, i.e., $Y = Y^1 \cup Y^2$. Herewith, we then obtain the periodic porous catalyst by covering Ω with respect to the reference pore Y where the periodic union of Y^1 forms the pore space Ω^ϵ and in the same way the periodic union of the solid phase Y^2 gives the solid matrix B^ϵ.

Based on the ORR reaction (1.1), this allows us to state the following microscopic equations, describing reactions and transport in a porous, completely water-filled catalyst layer of a PEM fuel cell. These equations represent water flow (incompressible Stokes flow), diffusion and convection of oxygen, and proton transport by diffusion, migration and convection. The electric field is largely determined by the distribution of protons and by the wall charge density σ^ϵ_s.

$$\begin{cases} -\epsilon^2\Delta \mathbf{u}^\epsilon + \nabla p^\epsilon = \kappa \mathbf{f}^\epsilon := -\kappa c^\epsilon_+ \nabla\phi^\epsilon & \text{in } \Omega^\epsilon, \\ \operatorname{div}\mathbf{u}^\epsilon = 0 & \text{in } \Omega^\epsilon, \\ \mathbf{u}^\epsilon_\tau = 0 & \text{on } \partial\Omega^\epsilon \setminus \left(E^\epsilon_+ \cup E^\epsilon_O\right), \\ \mathbf{u}^\epsilon_n = -\frac{\epsilon}{2} R_w(c^\epsilon_+, c^\epsilon_O, \eta^\epsilon) & \text{on } \partial\Omega^\epsilon \setminus \left(E^\epsilon_+ \cup E^\epsilon_O\right), \\ \mathbf{u}^\epsilon \text{and } p^\epsilon \text{periodic on } E^\epsilon_O \cup E^\epsilon_+, \end{cases} \tag{2.1}$$

$$\begin{cases} \partial_t c^\epsilon_O - \operatorname{div}\left(\mathbb{D}^O \nabla c^\epsilon_O - \mathrm{Pe}\mathbf{u}^\epsilon c^\epsilon_O\right) = 0 & \text{in } \Omega^\epsilon, \\ c^\epsilon_O = c^D_O & \text{on } E^\epsilon_O, \\ -\mathbf{n}\cdot\left(\mathbb{D}^O \nabla c^\epsilon_O - \mathrm{Pe}\mathbf{u} c^\epsilon_O\right) = 0 & \text{on } E^\epsilon_+, \\ -\mathbf{n}\cdot\left(\mathbb{D}^O \nabla c^\epsilon_O - \mathrm{Pe}\mathbf{u} c^\epsilon_O\right) = \frac{\epsilon}{4} R_O(c^\epsilon_+, c^\epsilon_O, \eta^\epsilon) & \text{on } I^\epsilon, \end{cases} \tag{2.2}$$

$$\begin{cases} \partial_t c^\epsilon_+ - \operatorname{div}\left(\mathbb{D}^+\left(\nabla c^\epsilon_+ + c^\epsilon_+ \nabla\phi^\epsilon\right) - \mathrm{Pe}\mathbf{u}^\epsilon c^\epsilon_+\right) = 0 & \text{in } \Omega^\epsilon, \\ -\mathbf{n}\cdot\left(\mathbb{D}^+\left(\nabla c^\epsilon_+ + c^\epsilon_+ \nabla\phi^\epsilon\right) - \mathrm{Pe}\mathbf{u}^\epsilon c^\epsilon_+\right) = 0 & \text{on } E^\epsilon_O, \\ c^\epsilon_+ = c^D_+ & \text{on } E^\epsilon_+, \\ -\mathbf{n}\cdot\left(\mathbb{D}^+\left(\nabla c^\epsilon_+ + c^\epsilon_+ \nabla\phi^\epsilon\right) - \mathrm{Pe}\mathbf{u}^\epsilon c^\epsilon_+\right) = \epsilon R_+(c^\epsilon_+, c^\epsilon_O, \eta^\epsilon) & \text{on } I^\epsilon, \end{cases} \tag{2.3}$$

$$\begin{cases} -\operatorname{div}\left(\mathbb{E}(\mathbf{x}/\epsilon)\nabla\phi^\epsilon\right) = c^\epsilon_+ & \text{in } \Omega^\epsilon, \\ \phi^\epsilon = \phi^D_O & \text{on } E^\epsilon_O, \\ \phi^\epsilon = \phi^D_+ & \text{on } E^\epsilon_+, \\ -\mathbf{n}\cdot\left(\mathbb{E}^\epsilon \nabla\phi^\epsilon\right) = \epsilon\sigma^\epsilon_s(\mathbf{x}) & \text{on } I^\epsilon. \end{cases} \tag{2.4}$$

The variable $\varepsilon(\mathbf{x}/\epsilon) := \lambda^2\chi_{\Omega^\epsilon}(\mathbf{x}/\epsilon) + \gamma\chi_{B^\epsilon}(\mathbf{x}/\epsilon)$ is Y-periodic for the dimensionless electric permittivity $\gamma := \frac{\varepsilon^s}{\varepsilon^p}$ where ε^s and ε^p (see Figure 1) stand for the electric permittivity of the solid and the pore phase, respectively. Moreover, $\lambda := \frac{\lambda_D}{L}$ represents the dimensionless form of the Debye length $\lambda_D := \left(\frac{\varepsilon^p RT}{2z_+^2 eF\bar{c}}\right)^{1/2}$ for a reference salt concentration $\bar{c}$ and a charge number z_+ of protons whose dimensionless density is denoted by c_+. This defines $\mathbb{E}^\epsilon := \{\varepsilon_{kl}\}_{1\le k,l\le N}$ by $\varepsilon_{kl} := \varepsilon(\mathbf{x}/\epsilon)\delta_{kl}$ where δ_{kl} is the Kronecker delta. As in 5, 18, we consider the case of sufficiently large overpotentials η^ϵ which justify the use of the *cathodic branch* of the Butler-Volmer equation, i.e., we apply the following reaction rates

$$R_\iota(c^\epsilon_+, c^\epsilon_O, \eta^\epsilon) := \beta_\iota\left(c^\epsilon_+\right)^{n_+}\left(c^\epsilon_O\right)^{n_O}\exp\left(-\alpha_c\eta^\epsilon\right), \tag{2.5}$$

for $\iota \in \{+, O, w\}$ and with the cathodic transfer coefficient α_c, the dimensionless concentrations c_+ and c_O, the dimensionless parameters $\beta_\iota := \frac{i_0 L}{4eD^\iota}$ for $\iota \in \{+, O\}$, $\beta_w = \frac{i_0 M_w}{\rho_w F}$, and the reaction orders $n_+ = n_{+,ox}$ and $n_O = n_{O,ox}$. The variable i_0 is the exchange current density. The diffusion constants D^ι represent a reference value associated with the diffusion tensors $\mathbb{D}^\iota := \{\delta^\iota_{kl}\}_{1\le k,l\le N}$, $\iota \in \{+, O\}$. Note that we follow Chan and Eikerling[5] regarding the over-potential $\eta := \phi^\epsilon - \phi_0$ which assumes, in fact, only non-positive values. In electrochemistry, ϕ^ϵ is generally referred to as an activation over-potential in relation to the equilibrium potential ϕ_0.

Our upscaling, or homogenization, of general microscopic catalyst layers makes use of a separation of scales which is a consequence of the strong heterogeneity, i.e. $\epsilon \ll 1$. Directly related to this separation is the following local equilibrium property:

A system depending on a flow velocity $\mathbf{U}$ *is in* local thermodynamic equilibrium (LTE) *if and only if*

$$0 = \frac{\partial}{\partial x_k}\mu_\iota - \mathrm{U}_k, \quad \textit{for} \quad 1 \le k \le N, \tag{2.6}$$

on the microscale Y*, where* $\iota \in \{O, +\}$, U_k *is the* k*-th velocity component of the upscaled fluid velocity* $\mathbf{U}$ *and* μ_ι *denotes the upscaled electrochemical potenials*

$$\mu_\iota := \begin{cases} \ln C_O & \text{if} \quad \iota = O, \\ \ln C_+ + z_+\Phi & \text{if} \quad \iota = +. \end{cases} \tag{2.7}$$

The validity of local thermodynamic equilibria has traditionally been a common assumption in the classical theory of non-equilibrium systems.[7] It means, for example, that constitutive equations hold true at small scales under non-equilibrium conditions at the macroscopic scale.

Remark 2.1. *(LTE) We note that the local thermodynamic equilibrium requires that equation (2.6) only holds on the level of each reference cell. That means, macroscopic (slow) quantities do not vary on the associated microscale (fast scale). LTE plays a crucial role in the homogenization of nonlinear problems.*[17-19] *Finally, we remark*

that every system that shows a scale separation of the form $\epsilon \ll 1$ *allows for the LTE approximation. This is no approximation anymore in the limit* $\epsilon \to 0$ *where the upscaled equations are found.*

We note that the thermodynamic equilibrium characterization (2.6) in the context of fluid flow represents a combined requirement of the chemical potential and the fluid velocity, see 9 for an example. However, we remark that a modified Nernst-Planck problem is introduced in 9 based on arguments from continuum mechanics and thermodynamics.

Upscaling of the Pore-scale Equations Toward a Macroscopic Porous Catalyst Layer Formulation

For the upscaling, we use systematic multiscale expansions as applied in homogenization theory.[3,11,14] For strongly heterogeneous media, i.e. $\epsilon \ll 1$, the multiscale solutions $v^\epsilon \in \{\mathbf{u}^\epsilon, c_O^\epsilon, c_+^\epsilon, \phi^\epsilon\}$ are well-approximated by expansions of the form

$$v^\epsilon(\mathbf{x}) = v(\mathbf{x}, \mathbf{x}/\epsilon) \approx V(\mathbf{x}, \mathbf{x}/\epsilon) + \epsilon v_1(\mathbf{x}, \mathbf{x}/\epsilon) + \mathcal{O}(\epsilon^2), \qquad [3.1]$$

where V denotes the upscaled variable. It can be rigorously proven that the formal ansatz (3.1) leads to rigorous error bounds of the form $\mathcal{O}(\epsilon^{1/2})$ in the context of weak solutions.[17] This approach takes reliably into account the pore geometry and systematically treats nonlinear terms which can still not be captured by volume averaging strategies, for instance. Upscaled formulations are of general interest due to two key features: (a) effective macroscopic equations allow for efficient and low-dimensional computations; (b) one obtains important knowledge about the influence of the microscale such as geometry or material properties on the macroscale.

The basic idea in the subsequent upscaling of the microscopic equations (2.1)–(2.4) lies in approximating its solution by a leading order expansion (3.1). This has already been done for the Stokes equation (2.1), see for instance section 1.4, p.16 in 11. It leads systematically to Darcy's law with a permeability tensor $\overline{\mathbb{K}} := \{\mathrm{k}_{kl}\}_{1\le k,l\le N}$ defined by the reference cell Y as follows

$$\mathrm{k}_{kl} := \mathcal{M}_{Y^1}\left(\mathrm{w}_l^k\right) := \frac{1}{|Y|}\int_{Y^1} \mathrm{w}_l^k \, d\mathbf{y}, \qquad [3.2]$$

where $\mathbf{w}^k := [\mathrm{w}_1^k, \mathrm{w}_2^k, \ldots, \mathrm{w}_N^k]'$ solves the periodic cell problem

$$\begin{aligned} -\Delta \mathbf{w}^k + \nabla_y q^k &= \mathbf{e}_k, \quad \text{in } Y^1, \\ \operatorname{div}_y \mathbf{w}^k &= 0, \quad \text{in } Y^1, \\ \mathbf{w}^k &= \mathbf{0}, \quad \text{on } \partial Y^1 \cap \partial Y^2, \\ \mathbf{w}^k,\ q^k &\quad \text{are } Y-\text{periodic}, \end{aligned} \qquad [3.3]$$

where $\mathbf{e}_k$ denotes the canonical/standard basis in Eucledian space $\mathbb{R}^N$. Herewith, we can write Darcy's law as follows

$$\begin{cases} \mathbf{U} = \mathbf{F} - \overline{\mathbb{K}}\nabla P, & \text{in } \Omega, \\ \operatorname{div} \mathbf{U} = 0, & \text{in } \Omega, \end{cases} \qquad [3.4]$$

where the upscaled force term $\mathbf{F}$ will be determined after upscaling the remaining equations. Hence, we briefly summarize the main steps of the upscaling methodology for the remaining problems (2.2)–(2.4): applying the representation (3.1) to the system (2.2)–(2.4) and collecting terms of equal order in ϵ leads to so-called reference cell problems in $\mathcal{O}(\epsilon^{-1})$, or more specifically

$$\xi_O^k : \begin{cases} -\operatorname{div}\left(\mathbb{D}^O \nabla \xi_O^k - \mathbf{e}_k\right) = 0 & \text{in } Y^1, \\ \mathbf{n} \cdot \left(\mathbb{D}^O \nabla \xi_O^k - \mathbf{e}_k\right) = 0 & \text{on } I_Y, \\ \xi_O^k \text{is } Y-\text{periodic and } \mathcal{M}_{Y^1}\left(\xi_O^k\right) = 0, \end{cases} \qquad [3.5]$$

$$\xi_+^k : \begin{cases} -\operatorname{div}\left(\mathbb{D}^+ \nabla \xi_+^k\right) = -\operatorname{div}\left(\mathbb{D}^+ \nabla \xi_\phi^k\right) & \text{in } Y^1, \\ \mathbf{n} \cdot \left(\mathbb{D}^+ \nabla \xi_+^k - \mathbb{D}^+ \nabla \xi_\phi^k\right) = 0 & \text{on } I_Y, \\ \xi_O^k \text{is } Y-\text{periodic and } \mathcal{M}_{Y^1}\left(\xi_O^k\right) = 0, \end{cases} \qquad [3.6]$$

$$\xi_\phi^k : \begin{cases} -\operatorname{div}\left(\mathbb{E}(\mathbf{y})\nabla \xi_\phi^k - \mathbf{e}_k\right) = 0, & \text{in } Y, \\ \xi_\phi^k \text{ is } Y-\text{periodic and } \mathcal{M}_Y\left(\xi_\phi^k\right) = 0, \end{cases} \qquad [3.7]$$

where $1 \le k \le N$ and the first-order terms are defined by the upscaled variable V in the form $v_1(\mathbf{x}, \mathbf{x}/\epsilon) = -\sum_{k=1}^N \xi_v^k(\mathbf{y}) \frac{\partial V}{\partial x_k}$. Moreover, we set $I_Y := \partial Y^1 \cap \partial Y^2$. This separation is justified since the cell problems for the leading order terms $V(\mathbf{x}, \mathbf{y})$ in (3.1), obtained by collecting terms of $\mathcal{O}(\epsilon^{-2})$, show that $V(\mathbf{x}) = V(\mathbf{x}, \mathbf{y})$. The upscaled equations in $\mathcal{O}(\epsilon^0)$ then read as follows

$$\begin{cases} U = C_+ \overline{\mathbb{M}}^+ \nabla \Phi - \overline{\mathbb{K}} \nabla P, \quad \text{in } \Omega, \\ \operatorname{div} U \\ \quad = -\frac{1}{2}\overline{\beta}_w (C_+)^{n_+} (C_O)^{n_O} \exp(-\alpha_c(\Phi - \Phi_0)), \quad \text{in } \Omega, \end{cases} \qquad [3.8]$$

$$\begin{cases} \theta \partial_t C_O - \operatorname{div}\left(\overline{\mathbb{D}}^O \nabla C_O - \mathrm{Pe} U C_O\right) \\ = \frac{1}{4}\overline{\beta}_O (C_+)^{n_+} (C_O)^{n_O} \exp(-\alpha_c(\Phi - \Phi_0)), \quad \text{in } \Omega, \end{cases} \qquad [3.9]$$

$$\begin{cases} \theta \partial_t C_+ - \operatorname{div}\left(\overline{\mathbb{D}}^+ \nabla C_+ + C_+ \overline{\mathbb{M}}^+ \nabla \Phi - \mathrm{Pe} U C_+\right) \\ \quad = \overline{\beta}_+ (C_+)^{n_+} (C_O)^{n_O} \exp(-\alpha_c(\Phi - \Phi_0)), \quad \text{in } \Omega, \end{cases} \qquad [3.10]$$

$$\left\{-\operatorname{div}\left(\overline{\mathbb{E}} \nabla \Phi\right) = \theta C_+ + Q_s \quad \text{in } \Omega, \right. \qquad [3.11]$$

where the porosity parameter θ has been introduced. Its value usually lies in the range $0.2-0.5$ and it has an impact on the flow and the kinetics by affecting the mobility and diffusion of ions and oxygen. These properties are determined by the effective porous media correction tensors $\overline{\mathbb{D}}^O := \{\mathrm{d}_{kl}^O\}_{1\le k,l\le N}$, $\overline{\mathbb{D}}^+ := \{\mathrm{d}_{kl}^+\}_{1\le k,l\le N}$ and $\overline{\mathbb{M}}^+ := \{\mathrm{m}_{kl}^+\}_{1\le k,l\le N}$ which, along with $\overline{\mathbb{E}}^+ := \{\varepsilon_{kl}\}_{1\le k,l\le N}$, are defined by

$$\begin{cases} \mathrm{d}_{kl}^O := \frac{1}{|Y|}\int_{Y^1} \left(\delta_{kl}^O - \delta_{kj}^O \frac{\partial \xi_O^l}{\partial y_j}\right) \mathrm{d}y, \\ \mathrm{d}_{kl}^+ := \frac{1}{|Y|}\int_{Y^1} \left(\delta_{kl}^+ - \delta_{kj}^+ \frac{\partial \xi_+^l}{\partial y_j}\right) \mathrm{d}y, \\ \mathrm{m}_{kl}^+ := \frac{1}{|Y|}\int_{Y^1} \left(\delta_{kl}^+ - \delta_{kj}^+ \frac{\partial \xi_\phi^l}{\partial y_j}\right) \mathrm{d}y, \\ \varepsilon_{kl} := \frac{1}{|Y|}\int_{Y^1} \left(\varepsilon_{kl}(y) - \varepsilon_{kj}(y) \frac{\partial \xi_\phi^l}{\partial y_j}\right) \mathrm{d}y, \end{cases} \qquad [3.12]$$

where we again applied Einstein's summation convention on free repeated indexes j. Moreover, $Q_s(x) := \frac{1}{|Y|}\int_{I^Y} \sigma_s(x, y)\, do(y)$ is the upscaled surface charge density σ_s, $\overline{\beta}_\iota := \frac{i_0 L \Lambda}{e \mathrm{D}_\iota} := \beta_\iota \frac{|I_Y|}{|Y|}$ and $\overline{\beta}_w := \frac{i_0 L}{e \mathrm{D}_+}\frac{|I_Y|}{|Y|} := \beta_w \Lambda$, are dimensionless numbers coupling the interfacial reactions to the bulk equations for $\iota \in \{+, O\}$, L is the characteristic length of the catalyst layer, and the parameters n_+ and n_O denote reaction orders.

We note that the appearance of a background charge Q_s in (3.11) is well-accepted in semiconductor theory. In fact, the homogenization theory gives a rigorous justification for it.[16,18] More striking is the appearance of the electric field as a driving force in a macroscopic Darcy law, Eq. (3.8). In essence, it represents a macroscopic electro-osmotic drag. Meanwhile, an explicit model is required to determine σ_s. One method is to relate the electric potential of protons ϕ^ϵ at the pore surface I^ϵ to the surface charge density σ_s, following the concept of *potential of zero charge*, as proposed by Chan and Eikerling.[5] Essentially, it assumes a relatively constant Helmholtz capacitance to derive a Robin boundary condition for ϕ^ϵ at I^ϵ.

Remark 3.1 (Porous Media Correction Tensors 3.12). *From classical homogenization theory (e.g. 6), it follows that the tensors (3.12) are symmetric, positive definite. Moreover, in the case of isotropic electric permeabilities, i.e.* $\varepsilon_{kl} := \varepsilon\delta_{kl}$, *and an isolating porous medium* ($\gamma \to \infty$, *see 16), it follows that the correctors* $\xi_O^k = \xi_+^k = \xi_\phi^k$ *solve the same reference cell problem. In the case where the reference cells form straight channels, one can compute these correctors analytically, see 2, 16.*

The main feature of the porous media tensors is their accurate description of anisotropic systems which most periodic catalyst layer structures represent. Carbon nanotube arrays and 3M's whisker structure[8] contain a main axis of orientation and exhibit periodicity in two dimensions only. These two examples would be the ideal candidates to compute porous media tensors and validate them against experimental data. This is beyond the scope of this contribution but planned future work.

Upscaling for Periodic and Strongly Convective Flows

Next, we restrict ourselves to periodic fluid flow exhibiting a dominant Péclet number. That means that the Coulomb force $f^\epsilon = -\kappa c_+^\epsilon \nabla\phi^\epsilon$ and the chemical reaction on the pore walls R_w, which induce local non-periodic effects, are negligibly small in comparison to a constant flow driven by $f^\epsilon = e_1$. The positive sign in front of e_1 defines a flow from the PEM to the GDL. This leads then to the following periodic flow problem

$$\begin{cases} -\mu\Delta_y u + \nabla_y p = e_1 & \text{in } Y^1, \\ \operatorname{div}_y(u) = 0 & \text{in } Y^1, \\ u = 0 & \text{on } I_Y, \\ u \text{ and } p \text{ are } Y-\text{periodic}. \end{cases} \quad [4.1]$$

The difference in the upscaling is the use of an adapted approximation (3.1), which accounts for the dominant flow in the asymptotic expansion by a so-called moving frame:

$$u^\epsilon(t,x) = u\left(t, x - \frac{v}{\epsilon}t, x/\epsilon\right) \approx U(t,x) + \sum_{i=1}^{\infty} \epsilon^i u_i\left(t, x - \frac{v}{\epsilon}t, x/\epsilon\right). \quad [4.2]$$

The reference cell problems, which are obtained by collecting the terms of $\mathcal{O}(\epsilon^{-1})$, have the following form

$$\xi_O^k : \begin{cases} -\operatorname{div}_y\left(\mathbb{D}^O\nabla_y\xi_O^k\right) - \mathrm{Pe}_{mic}(u(y)\cdot\nabla_y)\xi_O^k \\ \quad = \mathrm{v}^k - \mathrm{Pe}_{mic}\mathrm{u}^k & \text{in } Y^1, \\ n\cdot\left(\mathbb{D}^O\nabla_y\xi_O^k - \mathrm{Pe}_{mic}u(y)\xi_O^k\right) = 0 & \text{on } I_Y, \\ \xi_O^k \text{ is } Y-\text{periodic and } \mathcal{M}_{Y^1}\left(\xi_O^k\right) = 0, \end{cases} \quad [4.3]$$

$$\xi_+^k : \begin{cases} -\operatorname{div}_y\left(\mathbb{D}^+\nabla_y\xi_+^k\right) + \mathrm{Pe}_{mic}(u(y)\cdot\nabla_y)\xi_+^k \\ \quad = -\operatorname{div}_y\left(\mathbb{D}^+\nabla_y\xi_\phi^k\right) - \left(\mathrm{v}^k - \mathrm{Pe}_{mic}\mathrm{u}^k\right) & \text{in } Y^1, \\ n\cdot\left(\mathbb{D}^+\nabla_y\xi_+^k - \mathbb{D}^+\nabla_y\xi_\phi^k - \mathrm{Pe}_{mic}u(y)\xi_+^k\right) = 0 & \text{on } I_Y, \\ \xi_O^k \text{is } Y-\text{periodic and } \mathcal{M}_{Y^1}(\xi_O^k) = 0, \end{cases} \quad [4.4]$$

$$\xi_\phi^k : \begin{cases} -\operatorname{div}\left(\mathbb{E}(y)\nabla\xi_\phi^k - e_k\right) = 0, & \text{in } Y, \\ \xi_\phi^k \text{ is } Y-\text{periodic and } \mathcal{M}_Y(\xi_\phi^k) = 0. \end{cases} \quad [4.5]$$

At $\mathcal{O}(\epsilon^0)$, we obtain the upscaled equations showing so-called diffusion-dispersion relations (e.g. Taylor-Aris dispersion) through tensors which depend on u:

$$\begin{cases} \theta\partial_t C_O - \operatorname{div}\left(\overline{\mathbb{D}}^O(u)\nabla C_O\right) \\ \quad = \frac{1}{4}\overline{\beta}_O(C_+)^{n_+}(C_O)^{n_O}\exp\left(-\alpha_c(\Phi-\Phi_0)\right), & \text{in } \Omega, \end{cases} \quad [4.6]$$

$$\begin{cases} \theta\partial_t C_+ - \operatorname{div}\left(\overline{\mathbb{D}}^+(u)\nabla C_+ + C_+\overline{\mathbb{M}}^+\nabla\Phi\right) \\ \quad = \overline{\beta}_+(C_+)^{n_+}(C_O)^{n_O}\exp\left(-\alpha_c(\Phi-\Phi_0)\right), & \text{in } \Omega, \end{cases} \quad [4.7]$$

$$\left\{-\operatorname{div}\left(\overline{\mathbb{E}}\nabla\Phi\right) = \theta C_+ + Q_s\right. . \quad [4.8]$$

Here, the effective transport tensors $\overline{\mathbb{D}}^O(u) := \{\mathrm{d}_{kl}^O\}_{1\le k,l\le N}$, $\overline{\mathbb{D}}^+(u) := \{\mathrm{d}_{kl}^+\}_{1\le k,l\le N}$, $\overline{\mathbb{M}}^+ := \{\mathrm{m}_{kl}^+\}_{1\le k,l\le N}$, $\overline{\mathbb{E}}^+ := \{\varepsilon_{kl}\}_{1\le k,l\le N}$, which we refer to as *porous media tensors*, are defined as follows

$$\begin{cases} \mathrm{d}_{kl}^O := \frac{1}{|Y|}\int_{Y^1}\left(\delta_{kl}^O\left(1+\mathrm{Pe}_{loc}(\mathrm{v}_k-\mathrm{u}_k)\xi_O^l\right) - \delta_{kj}^O\frac{\partial\xi_O^l}{\partial y_j}\right)\mathrm{d}y, \\ \mathrm{d}_{kl}^+ := \frac{1}{|Y|}\int_{Y^1}\left(\delta_{kl}^O\left(1+\mathrm{Pe}_{loc}(\mathrm{v}_k-\mathrm{u}_k)\xi_O^l\right) - \delta_{kj}^+\frac{\partial\xi_+^{3_l}}{\partial y_j}\right)\mathrm{d}y, \\ \mathrm{m}_{kl}^+ := \frac{1}{|Y|}\int_{Y^1}\left(\delta_{kl}^+ - \delta_{kj}^+\frac{\partial\xi_\phi^{3_l}}{\partial y_j}\right)\mathrm{d}y, \\ \varepsilon_{kl} := \frac{1}{|Y|}\int_{Y^1}\left(\varepsilon_{kl}(y) - \varepsilon_{kj}(y)\frac{\partial\xi_\phi^{3_l}}{\partial y_j}\right)\mathrm{d}y, \end{cases} \quad [4.9]$$

where we again applied Einstein's summation convention on free repeated indexes.

Summary

For the first time, a multi-scale approach has been presented to scale up governing equations for the oxygen reduction reaction in microscale pores of cathode catalyst layers in PEM fuel cells. It yields macroscopic transport equations that include porous media tensors which are computed by solving the single-pore problem for a periodic pore structure.

Arguably, the derivation of a macroscopic Darcy's law and a macroscopic Butler-Volmer equation are the most important results of this procedure. The latter derivation is quite intuitive but Darcy's law includes nontrivial tensors, namely the permeability tensor and the mobility tensor.

For the limiting case of periodic and strongly convective flow, Darcy's law at the macro-level is replaced by a single-pore problem for the velocity at the micro-level that, in turn, enters the macroscopic equations for the remaining variables (C_O, C_+, Φ) via tensors. Herewith, we obtain systematically effective macroscopic transport equations by these porous media correction tensors (3.12) that reliably account for microscopic characteristics such as pore geometry, interfacial reactions, and surface charges.

The employed method is generic in the sense that it is applicable to other electrode geometries and reaction rates such as the full Butler-Volmer equation. The only requirement is the presence of a strong heterogeneity, i.e., $\epsilon \ll 1$, as well as the existence of a characteristic reference geometry which defines the microscale of the porous medium. The corresponding macroscopic transport equations are generally expected to retain their mathematical structure. However, recent work[20] demonstrates in the case of upscaling of ionic transport equations for symmetric electrolytes, that a new transport term emerges on the macroscale due to specific material properties on the microscale.

The next step will be to compare numerical results, based on the macroscopic transport equations (3.8)–(3.11), to experimental data. For this purpose, a periodic pore structure is required for which high-quality data can be obtained in situ and with small errors, meaning with small uncertainty. This is a formidable challenge but the ultra-thin catalyst layers produced by 3M,[8] might provide a good starting point.

List of Symbols

B^ϵ	solid phase
c_ι^ϵ	microscopic concentrations, $\iota \in \{O,+\}$
C_ι	upscaled concentrations, $\iota \in \{O,+\}$
F	Faraday constant
i_0	exchange current density
I^ϵ	pore walls in porous medium Ω
I_Y	pore walls in reference pore Y
ℓ	length scale of the reference pore Y
L	length scale of the porous medium Ω
M_w	molar mass of water
n_+, n_O	reaction orders
n	microscopic normal vector

N	upscaled normal vector
p	pressure in the microscale domain Ω^ϵ
P	upscaled pressure
Q_s	upscaled surface charge on pore walls
u^ϵ	microscopic fluid velocity
u^ϵ_τ, u^ϵ_n	tangential and normal projection of u^ϵ
U, U_k	upscaled fluid velocity and its components
w^k	periodic fluid velocity in reference cell Y
Y	microscale reference pore
Y^1, Y^2	microscale pore, solid phase
x, y	macro-, microscopic coordinates
$\mathbb{D}^\iota$	diffusion tensors
$\overline{\mathbb{D}}^\iota$	effective diffusion tensors
$\mathbb{E}^\epsilon$	composite electric permittivity tensor
$\overline{\mathbb{E}}^\epsilon$	effective electric permittivity tensor
$\overline{\mathbb{K}}$	effective permeability tensor
$\overline{\mathbb{M}}^+$	effective mobility tensor
α_c	cathodic transfer coefficient
β_ι	dimensionless exchange current density, $\iota \in \{O, +, w\}$
$\overline{\beta}_\iota$	effective dimensionless exchange current density, $\iota \in \{O, +, w\}$
ϵ	heterogeneity parameter
ε	dimensionless electric permittivity
ε^s, ε^p	electric permittivity of solid, pore phase
η	over-potential
ϕ	electrostatic potential
κ	dimensionless intensity of Coulomb force
λ	dimensionless Debye length
λ_D	Debye length
μ_ι	chemical potential for C_ι, $\iota \in \{O, +\}$
ρ_w	density of water
θ	porosity
σ_s	wall charge density
ξ^k_+, ξ^k_O, ξ^k_ϕ	first order correctors of c^ϵ_+, c^ϵ_O, ϕ^ϵ
Φ	upscaled electrostatic potential
Φ_0	upscaled equilibrium electric potential
Ω	macroscopic, porous catalyst layer
Ω^ϵ	pore phase
Λ	Lebesgue measure of pore wall

References

1. G. Allaire, A. Damlamian, and U. Hornung, "Two-scale convergence on periodic surfaces and applications," *In Proceedings of the International Conference on Mathematical Modelling of Flow through Porous Media (May 1995)*, pages 15–25, 1996.
2. J.-L. Auriault and J. Lewandowska, *Transp. Porous Med.*, **16**(1), 31 (1994).
3. A. Bensoussan, J.-L. Lions, and G. Papanicolaou, *Asymptotic Analysis for Periodic Structures*, North-Holland Publishing Company, North-Holland, Amsterdam, 1978.
4. K. Chan, *Modeling of ultrathin catalyst layers in polymer electrolyte fuel cells: proton transport and water management*, PhD thesis, Simon Fraser University, 2013.
5. K. Chan and M. Eikerling, *J. Electrochem. Soc.*, **158**(1), B18 (2011).
6. D. Cioranescu and P. Donato, *An Introduction to Homogenization*, Oxford University Press, 2000.
7. S. R. De Groot and P. Mazur, *Non-equilibrium Thermodynamics*, Dover Publications, pp. 22–23, 1984.
8. M. Debe, *Nature*, **486**, 43 (2012).
9. W. Dreyer, C. Guhlke, and R. Muller, *Phys. Chem. Chem. Phys.*, **15**, 7075 (2013).
10. A. Gully, H. Liu, S. Srinivasan, A. K. Sethurajan, S. Schougaard, and B. Protas, *J. Electrochem. Soc.*, **161**, E3066 (2014).
11. U. Hornung, *Homogenization and Porous Media*, Interdisciplinary Applied Mathematics, Springer, 1997.
12. IEA , *Energy Technology Perspectives 2012*, IEA, 2012.
13. J. Larminie and A. Dicks, *Fuel Cell Systems Explained*, Wiley, 2003.
14. C. C. Mei and B. Vernescu, *Homogenization Methods for Multiscale Mechanics*, World Scientific, 2010.
15. S. J. Paddison and R. Paul, *Phys.Chem.Chem.Phys.*, **4**, 1158 (2002).
16. M. Schmuck and M. Z. Bazant, "Homogenization of the Poisson-Nernst-Planck equations for ion transport in charged porous media," arXiv:1202.1916v1 (2012).
17. M. Schmuck, *ZAMM-Z. Angew. Math. Me.*, **92**(4), 304 (2012).
18. M. Schmuck and P. Berg, *Appl. Math. Res. Express.*, **2013**(1), 57 (2013).
19. M. Schmuck, M. Pradas, G. A. Pavliotis, and S. Kalliadasis, *Nonlinearity*, **26**(12), 3259 (2013).
20. M. Schmuck, *J. Math. Phys.*, **54**, 021504 (2013).
21. Y. Shao, J. Liu, Y. Wang, and Y. Lin, *J. Mater. Chem.*, **19**, 46 (2008).
22. G. M. Whitesides and G. W. Crabtree, *Science*, **315**, 796 (2007).
23. D. Wu, S. J. Paddison, and J. A. Elliott, *Energy Environ. Sci.*, **1**, 284 (2008).